Available online at www.sciencedirect.com
SCIENCE DIRECT
Journal of Catalysis 230 (2005) 255–268
JOURNAL OF CATALYSIS
www.elsevier.com/locate/jcat

On the radical cracking of *n*-propylbenzene to ethylbenzene or toluene over Sn/Al_2O_3–Cl catalysts under reforming conditions

Stéphanie Toppi [a,b,1], Cyril Thomas [a,*], Céline Sayag [a], Dominique Brodzki [a], Katia Fajerwerg [a], Fabienne Le Peltier [b,2], Christine Travers [b], Gérald Djéga-Mariadassou [a]

[a] *Laboratoire de Réactivité de Surface, UMR CNRS 7609, case 178, Université Pierre et Marie Curie, 4 Place Jussieu, 75252 Paris, France*
[b] *Institut Français du Pétrole, 1 et 4 Avenue de Bois-Préau, 92852 Rueil-Malmaison cedex, France*

Received 10 November 2004; accepted 24 November 2004

Abstract

Two series of chlorided-alumina-supported Sn catalysts were synthesized with different precursors, $SnCl_2$ or $SnBu_4$, and with various contents of Sn. The acidity of the catalysts including 0.2 wt% Sn was characterized by FTIR adsorption–desorption of 2,6-dimethylpyridine (Brønsted acidity) and pyridine (Lewis acidity) and compared with that of Al_2O_3–Cl. The catalytic activity of the synthesized materials was investigated for the transformation of *n*-propylbenzene under reforming conditions. The results show that the incorporation of Sn into Al_2O_3–Cl is not harmless. Neither the nature of the Sn precursor nor the content of Sn evenly affects the acidity and the distribution of the isomerized and cracked products. The correlation between the product distribution obtained for the transformation of *n*-propylbenzene and the acidity of the Al_2O_3–Cl and the $0.2Sn_{SnCl_2}/Al_2O_3$–Cl catalysts supports the formation of isopropylbenzene and benzene catalyzed by Brønsted acid sites via carbenium ion chemistry. In contrast, the production of toluene and ethylbenzene occurs via radical chemistry. The formation of these products is assumed to be catalyzed by Lewis acid sites with different strengths. The stability of the proposed radical intermediate species is consistent with the involvement of stronger Lewis acid sites in the production of toluene compared with those involved in that of ethylbenzene. The catalytic cycles responsible for the formation of toluene and ethylbenzene via radical pathways over an Al–O pair are reported. Finally, it is worth noting that benzene is always the major product of the cracked compounds.

Keywords: Chlorided-alumina-supported tin catalysts; Hydrodealkylation; FTIR; 2,6-Dimethylpyridine; Pyridine; Lewis acidity; Brønsted acidity; Mechanisms; $SnBu_4$; $SnCl_2$

1. Introduction

New environmental regulations on benzene content in gasoline require a crucial control of its formation in the course of the reforming process, provided that the feedstocks do not contain *n*-C_6. In this refining process, benzene is a side product of alkylaromatic hydrodealkylation. Typical reforming catalysts, which consist of platinum supported on a chlorided-alumina carrier with either tin or rhenium added as a promoter, are bifunctional catalysts [1–3]. One of the aims of the studies initiated by our group was to gain a better understanding of such a side reaction under reforming conditions and more particularly to determine whether hydrodealkylation reactions occurred preferentially on the metallic function or on the acidic one. To achieve this goal, model monofunctional catalysts were studied [4,5]. These studies showed that hydrodealkylation reactions effectively occurred on both functions. Moreover, we showed that the dispersion and the Sn promotion of the Pt metallic

* Corresponding author. Fax: +33 1 44 27 60 33.
E-mail address: cthomas@ccr.jussieu.fr (C. Thomas).
[1] Present address: Gaz de France, 361 Avenue du Président Wilson, 93211 Saint-Denis La Plaine cedex, France.
[2] Present address: Axens, 89 Bd Franklin Roosevelt, 92500 Rueil Malmaison, France.

0021-9517/$ – see front matter
doi:10.1016/j.jcat.2004.11.026

phase [4,5] and the addition of Cl to an alumina carrier [4] markedly influenced the selectivity of the hydrodealkylated compounds. In the latter work, the model catalysts consisted of Al_2O_3 and Al_2O_3–Cl. For Pt–Sn/Al_2O_3 catalysts, however, it has been reported that not only was Sn closely associated with Pt, as Pt_xSn_y alloys, but it also coexisted as nonreducible SnO_x species, either in contact with the Pt particles or isolated on the alumina carrier [6]. This observation led us to study model acidic chlorided-alumina-supported Sn catalysts, which we believe to be most representative of the acidic function of the typical reforming catalyst. Surprisingly, as far as we know, such catalysts have scarcely been studied [7,8]. In these studies, Kirszensztejn et al. [8] used a rather unusual approach to introduce chloride into their Al_2O_3–SnO_2 samples by reacting them with gas-phase CCl_2F_2/H_2 at 300 °C. It must be noted that this treatment led to the introduction of fluoride into the samples as well, and that fluoride strongly influences the acid–base properties of alumina [9–11]. The acid–base properties of chlorine-free [12–15] and chlorided [7,8] alumina modified by tin oxides have been reported. Overall, these studies concluded that the acidity of alumina-supported Sn catalysts decreases with increasing amounts of tin.

The aim of this work was to investigate the influence of Sn addition to Al_2O_3–Cl (Sn/Al_2O_3–Cl catalysts) on the acidity of the catalytic materials and their catalytic activity in the transformation of *n*-propylbenzene (*n*-PB) under reforming conditions. For this purpose, two series of Sn/Al_2O_3–Cl catalysts were synthesized with different Sn precursors. The results reveal striking differences in the acidity and the catalytic activity of the materials, depending on the nature of the Sn precursor. In addition, the change in the catalytic activity of Al_2O_3–Cl with tin addition from the $SnCl_2$ precursor could be correlated with acidity characterizations. The mechanisms of the formation of the hydrodealkylated compounds are also discussed.

2. Experimental

2.1. Catalyst preparation

The chlorided alumina material (1 wt% Cl) was prepared by impregnation of γ-Al_2O_3 (GOD 200; surface area 200 $m^2\,g^{-1}$, porous volume 0.6 $cm^3\,g^{-1}$) with an aqueous chlorhydric acid solution (1.2 wt% HCl, Merck) for 45 min with stirring at room temperature (RT). After filtering, the material was dried in air at 120 °C overnight and calcined in flowing air (1 $L\,h^{-1}\,g_{cat}^{-1}$) at 500 °C for 2 h.

Sn/Al_2O_3–Cl catalytic materials were prepared with either $SnCl_2$ or $SnBu_4$ as a precursor (Merck). These materials are referred to as $x\,Sn_{(Sn\ precursor)}/Al_2O_3$–Cl, where x is the Sn content (wt%) of the synthesized catalyst. It must be emphasized that, because of the obviously different natures of the precursors, different synthesis routes were used.

The synthesis of a series of Sn_{SnCl_2}/Al_2O_3–Cl materials, with various contents of Sn, was close to that performed for the chlorided alumina catalyst. After being in contact with HCl for 45 min at RT, an appropriate amount of $SnCl_2$, diluted in the 1.2 wt% HCl solution, was introduced. The solution was then maintained under stirring for 4 h at RT. After filtering, the catalyst was exposed to an aqueous solution of hydrogen peroxide for 30 min at RT to allow for the oxidation of Sn^{II} to Sn^{IV}. The catalyst was then filtered and washed with distilled water and finally dried in air at 120 °C for 12 h. The decomposition of the Sn precursor was performed in air (1 $L\,h^{-1}\,g_{cat}^{-1}$) at 520 °C for 2 h. The H_2O_2 oxidation step was performed to allow for comparison with the catalysts synthesized with $SnBu_4$; the oxidation state of Sn in the latter series was Sn^{IV}.

The synthesis of the Sn_{SnBu_4}/Al_2O_3–Cl series of catalysts differed substantially from that of the Sn_{SnCl_2}/Al_2O_3–Cl series. Solutions of $SnBu_4$ in *n*-heptane (Aldrich), containing appropriate amounts of $SnBu_4$, were dripped into the Al_2O_3 support and kept for 1 h under continuous stirring at RT. *n*-C_7 was then evaporated under air at 120 °C for 15 h. The decomposition of the Sn precursor was performed in air (1 $L\,h^{-1}\,g_{cat}^{-1}$) at 150, 350 and 520 °C for 2 h at each temperature. The catalyst was then acidified with the same procedure as that used for Al_2O_3–Cl and Sn_{SnCl_2}/Al_2O_3–Cl, except that the catalyst was kept in contact with the solution for 24 h under stirring at RT. After filtering, the material was dried in air at 120 °C for 12 h and calcined in flowing air (1 $L\,h^{-1}\,g_{cat}^{-1}$) at 520 °C for 2 h.

Prior to catalytic measurements, the catalysts were calcined in situ in flowing air (1 $L\,h^{-1}\,g_{cat}^{-1}$) at 500 °C for 2 h and then reduced in H_2 (1 $L\,h^{-1}\,g_{cat}^{-1}$) at 500 °C for 2 h. The composition of the synthesized catalysts is listed in Table 1. This table shows that the applied protocols allowed for the preparation of the desired catalysts. Al_2O_3–Cl and Sn_{SnCl_2}/Al_2O_3–Cl catalysts contained 1 ± 0.1 wt% Cl. Note that the Sn_{SnBu_4}/Al_2O_3–Cl series of catalysts contained slightly lower amounts of Cl (0.8–0.9 wt%) than that the Al_2O_3–Cl and Sn_{SnCl_2}/Al_2O_3–Cl catalysts did. The two 0.2Sn/Al_2O_3–Cl catalysts exhibited identical Sn (0.19 wt%) and Cl (0.9 wt%) contents.

Table 1
Composition of the synthesized catalysts determined after calcination (air, 500 °C, 2 h) and subsequent reduction (H_2, 500 °C, 2 h)

Catalysts	Sn precursor	Cl (wt%)	Sn (wt%)
Al_2O_3–Cl	–	1.0	–
$0.1Sn_{SnCl_2}/Al_2O_3$–Cl	$SnCl_2$	1.0	0.13
$0.2Sn_{SnCl_2}/Al_2O_3$–Cl	$SnCl_2$	0.9	0.19
$0.5Sn_{SnCl_2}/Al_2O_3$–Cl	$SnCl_2$	1.1	0.48
$0.1Sn_{SnBu_4}/Al_2O_3$–Cl	$SnBu_4$	0.8	0.11
$0.2Sn_{SnBu_4}/Al_2O_3$–Cl	$SnBu_4$	0.9	0.19
$0.4Sn_{SnBu_4}/Al_2O_3$–Cl	$SnBu_4$	0.8	0.40

2.2. Characterization of the catalysts

2.2.1. Adsorption–desorption of probe molecules followed by infrared spectroscopy (FTIR)

FTIR spectra of adsorbed probe molecules on Al_2O_3–Cl and 0.2Sn/Al_2O_3–Cl were collected on a Bruker Vector 22 FTIR spectrometer equipped with a DTGS detector and a data acquisition station. The sample was pressed into a self-supporting wafer of 8–12 mg cm^{-2}. The wafer was loaded into a conventional pyrex glass cell sealed with KBr windows that was connected to a vacuum system, which produced a dynamic vaccum of at least 5×10^{-8} bar. Prior to adsorption of the probe molecules, the catalyst was submitted to oxidizing and reducing pretreatments at atmospheric pressure identical to those described in Section 2.1. After pretreatment, the catalyst was evacuated at 120 °C to remove residual traces of water. The catalyst temperature was then decreased to RT under dynamic vacuum (5×10^{-8} bar). Pyridine and 2,6-dimethylpyridine (2,6-DMP) were dried in vacuo and stored in the presence of a 3A molecular sieve. Pyridine and 2,6-DMP were adsorbed at RT under saturated atmospheres of the probe molecules. After being exposed to the probe molecules for 1.5 h, the catalysts were evacuated at 25, 150, and 300 °C for 15 min, and the FTIR spectra were recorded at RT; 128 scans were accumulated with a spectral resolution of 4 cm^{-1}. The spectrum of the pretreated catalyst was used as a reference and subtracted from the spectra of the catalysts exposed to the probe molecules, which were subsequently evacuated at different temperatures.

As already discussed in a previous paper from our laboratory [9], we followed the Lewis acidity by observing the area of the pyridine band at ca. 1450 cm^{-1}, assigned to pyridine coordinated with Lewis acid sites (L-Py, υ C–N or υ19b) [11,16]. Because of the low intrinsic Brønsted acidity of alumina materials, pyridine is not the most suitable probe molecule for characterizing Brønsted acid sites [11]. Therefore we followed the Brønsted acidity by observing the adsorption bands from 1650 to 1615 cm^{-1} attributed to the υ C–C vibration of the 2,6-DMP protonated probe molecule, as shown by Corma et al. [10,11].

The amount of Lewis and Brønsted acid sites (a.u.) reported in the present work was normalized to a disk of 5 mg cm^{-2}. Given that the extinction coefficients were not determined, Lewis and Brønsted acidities could not be quantitatively compared with each other.

2.2.2. Catalytic activity

Catalytic measurements were carried out with commercial *n*-propylbenzene (Fluka, purum $\geqslant$ 98%) as a reactant without further purification. Liquid *n*-propylbenzene was delivered to the catalytic device [4,5] with a high-pressure piston pump (Gilson 307). The hydrogen flow and the total pressure were controlled with a mass-flow controller (Brooks 5850 TR) and a back-pressure regulator (Brooks 5866), respectively.

Blank experiments, in which the reactor contained no catalyst, indicate that thermal cracking was negligible compared with that observed in the presence of the catalysts. Reactions were carried out with 0.8 g of catalyst (0.16–0.20 mm) in a fixed-bed microreactor, at a temperature of 500 °C and a total pressure of 5 bars. Catalytic measurements were performed on stabilized catalysts. The contact time varied from 0.8 to 2.8 s, during which a hydrogen/hydrocarbon molar ratio of 5 was maintained. The reaction products were analyzed with an on-line gas chromatograph (HP 4890, FID), and the identification of the products was confirmed by GC-MS (HP 5890-HP 5971A) analysis and injection of the standards. GC and GC-MS analyses were performed with a PONA (Paraffins–Olefins–Naphtenes–Aromatics) capillary column (Hewlett–Packard, 50 m long, inner diameter 0.20 mm, film thickness 0.5 μm).

3. Results

3.1. Adsorption–desorption of probe molecules followed by FTIR spectroscopy

3.1.1. Adsorption of 2,6-dimethylpyridine

Fig. 1 shows infrared spectra for 2,6-DMP, adsorbed at RT, after desorption at 25, 150, and 300 °C under vacuum over Al_2O_3–Cl and 0.2Sn/Al_2O_3–Cl. Adsorption bands at 1580 cm^{-1} and about 1600 cm^{-1}, assigned to the interaction of 2,6-DMP with Brønsted acid sites [10,11], rapidly decrease with increasing desorption temperature, except for the 0.2Sn_{SnCl_2}/Al_2O_3–Cl catalyst (Fig. 1b). Over Al_2O_3–Cl (Fig. 1a) and 0.2Sn_{SnCl_2}/Al_2O_3–Cl (Fig. 1b), adsorption bands in the 1615–1640 cm^{-1} region are less affected by the desorption treatment than the 1650 cm^{-1} band, which rapidly vanishes upon desorption. For these two catalysts, a shift of the 1615 cm^{-1} band to higher frequency is observed. As already suggested by Corma et al. [10], considering a wide distribution of OH groups with different acid strengths, an increase in the desorption temperature provokes the desorption of 2,6-DMP, starting from the weakest (lower frequency) acid centers, and shifts the 1615 cm^{-1} band toward higher frequencies (strongest acid centers).

Table 3 lists the Brønsted acid site distributions, as deduced from the 1615–1650 cm^{-1} adsorption bands (Table 2). It is worth emphasizing that the introduction of Sn via $SnCl_2$ significantly increases the total amount of Brønsted acid sites, whereas that via $SnBu_4$ decreases it very slightly. The distribution of the Brønsted acid sites is also strongly affected by $SnCl_2$, with a significant increase in the amounts of both weak and strong acid centers and a decrease in that of the medium acid sites. Conversely, the distribution of the Brønsted acid centers is scarcely affected when $SnBu_4$ is used as a Sn precursor (Figs. 1a and 1c).

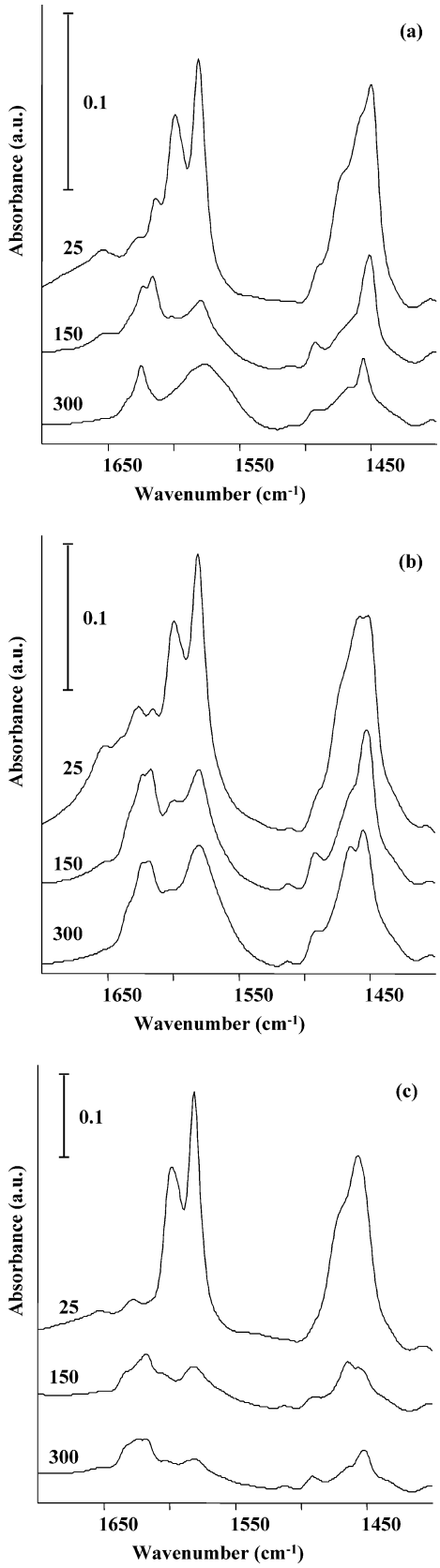

Fig. 1. Infrared spectra of adsorbed 2,6-dimethylpyridine on calcined (air, 500 °C, 2 h) and reduced (H_2, 500 °C, 2 h) catalysts with increasing evacuation temperature: (a) Al_2O_3–Cl, (b) $0.2Sn_{SnCl_2}/Al_2O_3$–Cl, and (c) $0.2Sn_{SnBu_4}/Al_2O_3$–Cl.

3.1.2. Adsorption of pyridine

Infrared spectra of the Al_2O_3–Cl and the $0.2Sn/Al_2O_3$–Cl samples, taken after adsorption of pyridine at RT and further desorption under vacuum at various temperatures, are given in Fig. 2. In agreement with a previous work [11], adsorption bands of pyridine coordinated to Lewis acid sites can be seen at 1450, 1500, and 1580 cm^{-1}. For all catalysts, the intensities of these bands decrease with increasing desorption temperature. A shift of these bands to higher wavenumbers is also observed with increasing desorption temperature. The same explanation as that mentioned in the case of 2,6-DMP can be given to account for this shift. The total amount of Lewis acid sites and the distribution of their strength were estimated with reference to the adsorption band at ca. 1450 cm^{-1} (Table 3). The introduction of Sn leads to a decrease in the total amount of Lewis acid sites for both $0.2Sn/Al_2O_3$–Cl catalysts. Nevertheless, this decrease is more pronounced for the catalyst synthesized from $SnBu_4$ than that synthesized from $SnCl_2$. For all catalysts, the amount of weak Lewis acid sites is always the greatest; the $0.2Sn_{SnCl_2}/Al_2O_3$–Cl catalyst exhibits the greatest amount of weak Lewis acid sites, followed by Al_2O_3–Cl. The amount of medium Lewis acid sites decreases with the incorporation of Sn. This effect is the more pronounced for the $0.2Sn_{SnCl_2}/Al_2O_3$–Cl sample. Finally, the amount of strong Lewis acid sites is slightly lower over the supported Sn catalysts compared with that over Al_2O_3–Cl.

3.2. Catalytic activity

3.2.1. Sn_{SnCl_2}/Al_2O_3–Cl catalysts

The formation rates of the isomerized and hydrodealkylated products (isopropylbenzene, benzene, toluene, ethylbenzene + styrene) of *n*-propylbenzene under reforming conditions, on the Sn_{SnCl_2}/Al_2O_3–Cl catalysts, are listed in Table 4. The addition of Sn promotes the formation of isopropylbenzene and that of the sum of ethylbenzene and styrene. The promotional effect of Sn on the formation of isopropylbenzene, nevertheless, is greater than that on the sum of ethylbenzene and styrene. For both products, a maximum beneficial effect of Sn is obtained for a content of 0.2 wt% Sn. The incorporation of Sn also promotes the formation of benzene for Sn contents equal or lower than 0.2 wt%. In this case, however, a monotonous decrease in the formation rate of benzene is observed with increasing Sn contents. Conversely, the formation of toluene is not favored by the addition of Sn, and its formation rate decreases monotonously with increasing Sn content.

Fig. 3 shows the formation of these products as a function of contact time over $0.2Sn_{SnCl_2}/Al_2O_3$–Cl. The formation of isopropylbenzene, toluene, and the sum of ethylbenzene and styrene extrapolates to positive axis ordinate intercepts, whereas that of benzene extrapolates to a negative axis ordinate intercept (Fig. 3). In agreement with Best and Wojciechowski [17], these results suggest that isopropylbenzene, toluene, and the sum of ethylbenzene and styrene

Table 2
FTIR characterization of Brønsted and Lewis acid sites of Al_2O_3–Cl, $0.2Sn_{SnCl_2}/Al_2O_3$–Cl and $0.2Sn_{SnBu_4}/Al_2O_3$–Cl. Absorbances (per Unit Surface Area) of the 1615–1650 cm^{-1} bands of 2,6-dimethylpyridine (2,6-DMP) and of the 1450 cm^{-1} band of pyridine adsorbed on the catalysts, after desorption at different temperatures

Catalysts	Absorbances					
	2,6-DMP (Brønsted acid sites)			Pyridine (Lewis acid sites)		
Desorption temperature (°C)	25	150	300	25	150	300
Al_2O_3–Cl	2.16	1.54	0.73	3.88	1.90	1.00
$0.2Sn_{SnCl_2}/Al_2O_3$–Cl	3.87	2.26	1.76	3.56	1.34	0.90
$0.2Sn_{SnBu_4}/Al_2O_3$–Cl	2.07	1.73	0.71	3.07	1.64	0.94

Table 3
Influence of the nature of the Sn precursor on the distribution of the acid sites as a function of the desorption temperature ($T_{des.}$), as deduced from FTIR measurements reported in Table 2

	Acid site distribution		
	Al_2O_3–Cl	$0.2Sn_{SnCl_2}/Al_2O_3$–Cl	$0.2Sn_{SnBu_4}/Al_2O_3$–Cl
Brønsted acid sites			
Weak ($25 > T_{des.} > 150$ °C)	0.62	1.61	0.34
Medium ($150 > T_{des.} > 300$ °C)	0.81	0.50	1.02
Strong ($T_{des.} > 300$ °C)	0.73	1.76	0.71
Brønsted total	2.16	3.87	2.07
Lewis acid sites			
Weak ($25 > T_{des.} > 150$ °C)	1.98	2.22	1.43
Medium ($150 > T_{des.} > 300$ °C)	0.90	0.44	0.70
Strong ($T_{des.} > 300$ °C)	1.00	0.90	0.94
Lewis total	3.88	3.56	3.07

Table 4
Influence of the Sn content on the formation rates of isopropylbenzene and hydrodealkylated compounds (benzene, toluene and the sum of ethylbenzene and styrene) for catalysts synthesized with $SnCl_2$ as precursor

Formation rate[a] (10^{-5} mol L^{-1} s^{-1})	Catalysts			
	Al_2O_3–Cl	$0.1Sn_{SnCl_2}/Al_2O_3$–Cl	$0.2Sn_{SnCl_2}/Al_2O_3$–Cl	$0.5Sn_{SnCl_2}/Al_2O_3$–Cl
Isopropylbenzene	3.0	16.6	20.8	13.0
Benzene	9.8	13.9	12.0	5.6
Toluene	2.9	2.5	2.2	1.3
Ethylbenzene + styrene	2.3	3.5	3.6	2.7

[a] Data recorded for 5 h of run.

Table 5
Influence of the Sn content on the formation rates of isopropylbenzene and hydrodealkylated compounds (benzene, toluene and the sum of ethylbenzene and styrene) for catalysts synthesized with $SnBu_4$ as precursor

Formation rate[a] (10^{-5} mol L^{-1} s^{-1})	Catalysts			
	Al_2O_3–Cl	$0.1Sn_{SnBu_4}/Al_2O_3$–Cl	$0.2Sn_{SnBu_4}/Al_2O_3$–Cl	$0.4Sn_{SnBu_4}/Al_2O_3$–Cl
Isopropylbenzene	3.0	3.1	1.9	2.9
Benzene	9.8	6.7	5.2	3.2
Toluene	2.9	2.4	1.7	1.3
Ethylbenzene + styrene	2.3	3.7	3.2	2.8

[a] Data recorded for 5 h of run.

are primary products, whereas benzene is a stable secondary product. It is also interesting to note that the formation of isopropylbenzene flattens at high contact time (Fig. 3, 2.8 s). This behavior is typical of an unstable primary product that further transforms into a secondary product [17]. These observations, described for the $0.2Sn_{SnCl_2}/Al_2O_3$–Cl catalyst, also hold for Al_2O_3–Cl and Sn_{SnBu_4}/Al_2O_3–Cl catalysts, although they are less pronounced than for the Sn_{SnCl_2}/Al_2O_3–Cl series of catalysts, because of lower conversions with the former materials.

3.2.2. Sn_{SnBu_4}/Al_2O_3–Cl catalysts

Table 5 lists the formation rates of the isomerized and hydrodealkylated products of *n*-PB with increasing Sn content of the Sn_{SnBu_4}/Al_2O_3–Cl catalysts. Whereas the introduction of Sn from $SnCl_2$ has a significant influence on the formation of the isomerized and hydrodealkylated products, Sn incorporation from $SnBu_4$ has less influence on the catalytic transformation of *n*-PB over these catalysts. The formation of isopropylbenzene is roughly constant throughout the series of catalysts, whereas that of benzene and toluene decreases monotonically with increasing Sn content. On the other hand, the formation of ethylbenzene and styrene is promoted slightly by the incorporation of Sn, but decreases as the amount of Sn increases.

4. Discussion

4.1. Formation of isopropylbenzene and benzene

Tables 3–5 show that the introduction of Sn from different precursors does not evenly affect the acidity of the chlorided alumina catalyst and the formation of isopropylbenzene and benzene. It is obvious from Table 3 that the addition of 0.2 wt% Sn from $SnCl_2$ enhances Brønsted acidity with a marked increase in the amount of strong and weak acid sites compared with Al_2O_3–Cl, whereas the Brønsted acidity of $0.2Sn_{SnBu_4}/Al_2O_3$–Cl scarcely differs from that of Al_2O_3–Cl. Moreover, the incorporation of Sn from both precursors only slightly decreases the Lewis acidity of the supported Sn catalysts compared with that of the chlorided alumina material. It is also interesting to note that the supported Sn catalysts synthesized from $SnCl_2$ drastically enhance the formation of isopropylbenzene and benzene,

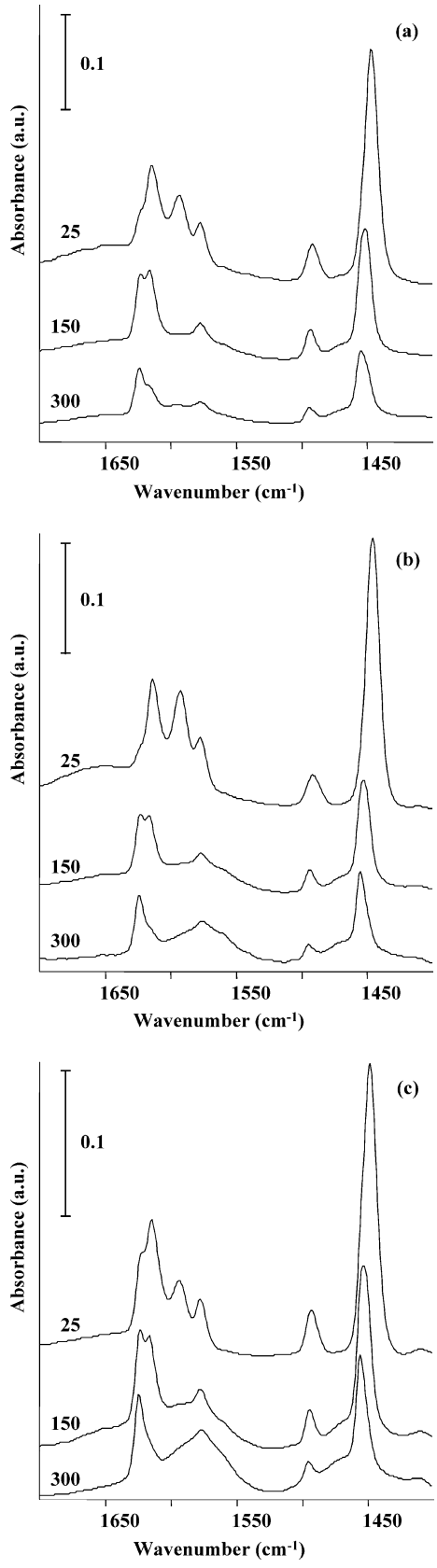

Fig. 2. Infrared spectra of adsorbed pyridine on calcined (air, 500 °C, 2 h) and reduced (H_2, 500 °C, 2 h) catalysts with increasing evacuation temperature: (a) Al_2O_3–Cl, (b) $0.2Sn_{SnCl_2}/Al_2O_3$–Cl, and (c) $0.2\ Sn_{SnBu_4}/Al_2O_3$–Cl.

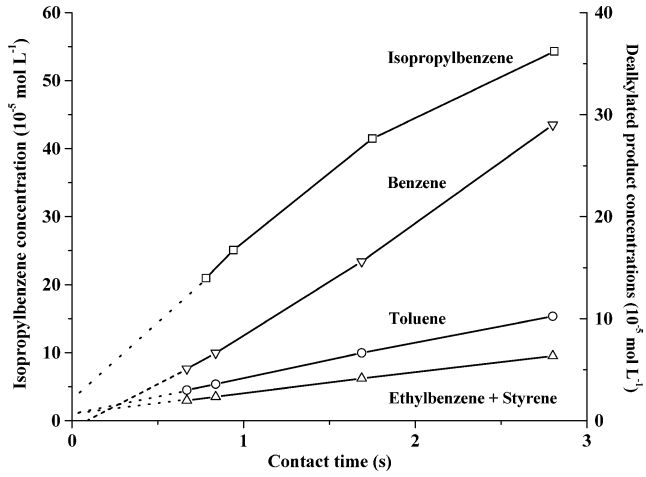

Fig. 3. Concentrations of isopropylbenzene, benzene, toluene and the sum of ethylbenzene and styrene versus contact time, in the conversion of *n*-propylbenzene at 500 °C, 5 bars, and $H_2/HC = 5$ over $0.2Sn_{SnCl_2}/Al_2O_3$–Cl (extrapolated values: dotted lines). Data recorded for 5 h of run.

although this only occurs up to 0.2 wt% Sn for benzene (Table 4), whereas the formation of isopropylbenzene is not affected by the introduction of Sn from $SnBu_4$, and the formation of benzene decreases with $SnBu_4$ addition (Table 5). The correlation between FTIR characterization of the acidic properties and the reactivity of the $0.2Sn/Al_2O_3$–Cl catalysts supports the formation of isopropylbenzene and benzene catalyzed by the Brønsted acid sites. In addition, the profile concentration of these products as a function of contact time suggests that *n*-PB first isomerizes to isopropylbenzene before cracking to benzene (Fig. 3). The formation of benzene from *n*-PB is shown in Fig. 4. Dehydrogenated products of *n*-PB, already reported in a previous study over alumina catalysts [4], are also detected over the supported tin catalysts (not shown). However, the formation of these compounds is not the aim of the present section and will be discussed later (Section 4.2.3); hence their formation from *n*-PB is symbolized by a catalytic cycle in which the nature of the involved acid sites is assumed to be a Lewis acid site (top of Fig. 4). In Fig. 4, it is assumed that dehydrogenated products of *n*-PB are protonated to a benzylic carbenium ion; this cation is the most stable, as it is resonantly stabilized by the aromatic nucleus. This benzylic carbenium ion then isomerizes to an isopropylbenzene carbenium ion either via a protonated cyclopropane intermediate or via a methyl shift [18]. It is noteworthy that this isomerization step leads to a primary carbenium ion, the formation of which is known to be highly unfavored [18,19]. However, in this particular case, this primary carbenium ion might readily isomerize to the corresponding highly stable tertiary isopropylbenzene carbenium ion via a 1,2 hydrogen atom shift; such carbenium ion rearrangements have indeed been reported as facile [20]. The hydride transfer [18,19] from a *n*-PB molecule yields to isopropylbenzene and a benzylic carbenium ion; the latter intermediate allows the izomerization cycle to turn over.

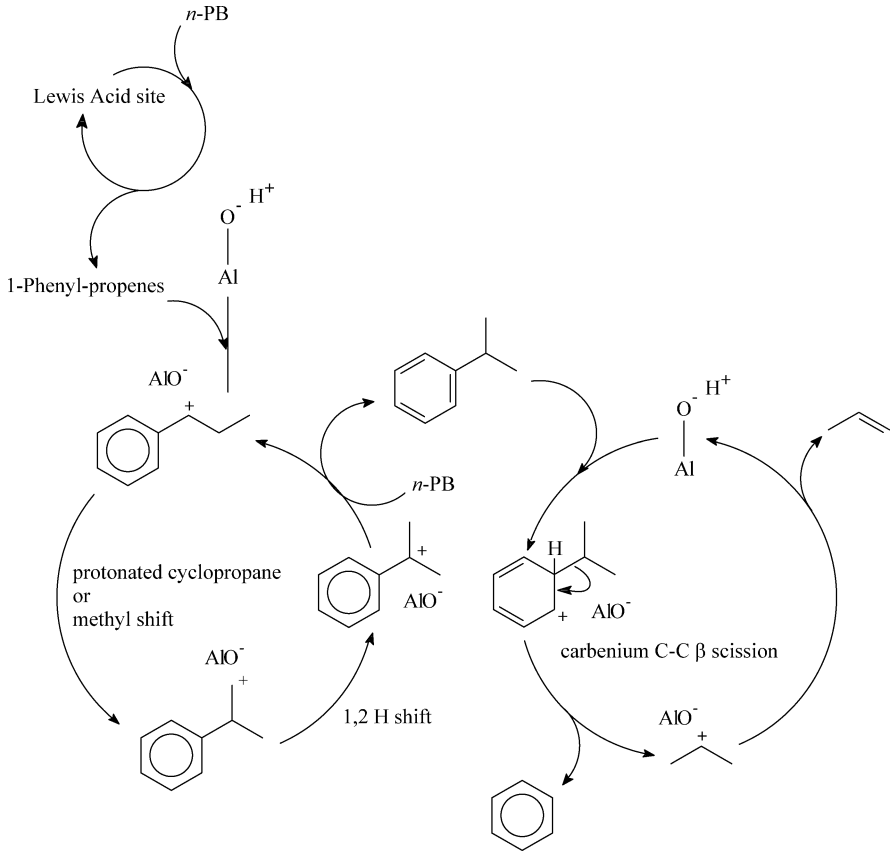

Fig. 4. Carbenium-ion cracking of benzene catalyzed by Brønsted acid sites.

The cracking of isopropylbenzene has largely been studied in the literature as a model reaction to characterize the strength of the sites of acidic catalysts [21–25]. It is generally accepted that the cracking of isopropylbenzene is catalyzed by Brønsted acid sites [23–25] by protonation of the ipso position of the aromatic nucleus [25] to yield the protonated benzene ring carbenium ion (catalytic cycle on the right side of Fig. 4). A classic C–C β scission of this carbenium ion leads to benzene and propene after the loss of a proton from the isopropyl carbocation. Based on the aforementioned possible carbenium ion 1,2 H atom shift rearrangement in the case of the isomerization of *n*-PB, one might also consider the direct C–C bond scission of the linear alkyl chain group of *n*-PB. This β scission would yield to benzene and a primary carbenium propyl ion; the subsequent rearrangement of the latter to an isopropyl cation and the loss of a proton also leads to propene. However, benzene appears as a stable secondary product and isopropylbenzene appears as an unstable primary product (Fig. 3, [17]). The mechanism reported in Fig. 4 for the formation of benzene is therefore the more likely. Moreover, this mechanism is in good agreement with the cracking of linear alkanes, for which isomerization steps are known to precede C–C β scissions to avoid the intermediate formation of primary carbenium ions [18]. Finally, it is worth mentioning that for poorly acidic catalysts, such as Al_2O_3, a radical cracking of isopropylbenzene was also suggested to occur to a significant extent [22].

4.2. Formation of toluene and ethylbenzene

4.2.1. Carbenium-ion chemistry

If the formation of isopropylbenzene and benzene might be reasonably attributed to carbenium ion chemistry, there is a possible rebuttal to the formation of toluene and ethylbenzene and thus styrene, which is the dehydrogenated analog of ethylbenzene, via classic C–C β scissions of carbenium ion chain mechanisms.

The only carbenium ion that allows for the formation of ethylbenzene is the benzylic carbocation that is also involved in the isomerization catalytic cycle (catalytic cycle on the left side of Fig. 4). It is obvious that the C–C β scission of such a carbenium ion leads to the formation of styrene and a methenium ion (CH_3^+) [4], with the rather doubtful formation of the latter from a thermodynamic point of view, ruling out the involvement of a carbenium ion mechanism for the formation of ethylbenzene.

On the other hand, it is worth considering the possibility of the formation of toluene via a rather complex transformation of a carbenium ion produced by protonation of the benzene ring at the ortho position [4]. In such an eventuality, the formation of toluene occurs together with the formation of a primary ethylene carbenium ion ($^+CH_2$–CH_3). However, this carbenium ion cannot rearrange to a more stable carbenium ion, as was the case in the isomerization process of *n*-PB (Section 4.1, catalytic cycle on the left side of

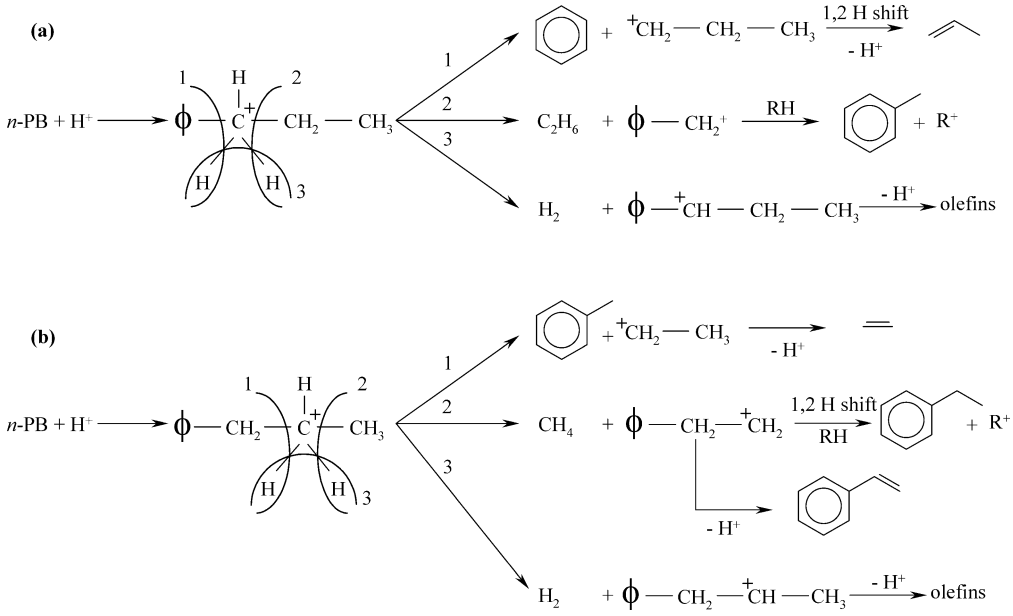

Fig. 5. Protolytic cracking of *n*-PB via penta-coordinated carbonium ions adapted from the work of Haag and Dessau [32].

Fig. 4). Although the stability of such a primary carbenium ion might be greatly questionable, it is well known that alkylation of benzene by ethylene occurs over acidic catalysts [26,27], suggesting that these materials are able to stabilize the ethylene primary carbenium ion. It is generally accepted that the mechanism of aromatic alkylation takes place via a carbenium ion, as the formation of the latter results from the activation of olefin by Brønsted acid sites [16,27]. The associated base of the Brønsted acid sites catalyzing the alkylation reaction is therefore able to stabilize the ethylene carbenium ion and hence performs the same role for the reverse reaction of benzene alkylation (i.e., ethylbenzene dealkylation). In the present work, a similar path could be considered for the hydrodealkylation of *n*-PB to toluene with the stabilization of an ethylene carbenium ion. Nevertheless, one can observe that the Brønsted acidity of $0.2Sn_{SnCl_2}/Al_2O_3$–Cl increases sharply compared with Al_2O_3–Cl (Table 3), and the formation of toluene decreases (Table 4). This suggests that, in the present study, Brønsted acid sites do not catalyze the production of toluene via a carbenium ion chain mechanism.

4.2.2. Carbonium ion chemistry

As reported above, none of the existing C–C bond fission schemes based on carbenium ion chemistry can easily account for the formation of ethylbenzene and toluene in the present study. Similarly, Notari et al. [28] stated that the carbenium ion mechanism could not be applied for the hydrodealkylation of methyl- and ethyl-substituted aromatics. Such a conclusion has also been drawn in previous works [18,20,29–31] that focused on the cracking of small molecules, such as *n*-butane or *i*-butane, to C_1–C_3 products over acidic catalysts. Indeed, the cracking of *n*-butane via a carbenium ion mechanism implies the formation of a methenium ion for the formation of C_1 and C_3 compounds or a primary carbenium ion for C_2 products. Another strikingly obvious difficulty is that the dominant carbenium ion derived from *i*-butane does not have a β_C–C bond. To overcome these difficulties, Haag and Dessau originally suggested the existence of a carbonium mechanism also referred to as protolytic cracking [32]. This mechanism involves the direct protonation of the alkane molecule by very strong Brønsted acid sites to form a pentacoordinated carbonium ion ($^+C_xH_{2x+3}$). The decomposition of this carbonium ion with the cleavage of α bonds results in the formation of C_1–C_3 light alkanes and carbenium ions that further transform into olefins with the loss of protons.

The main argument against the formation of toluene via protolytic cracking has already been stated above (Section 4.2.1). Indeed, it is difficult to conceive that toluene production takes place via a carbonium ion mechanism as its formation rate decreases (Table 4) with the introduction of 0.2 wt% Sn to Al_2O_3–Cl, whereas the Brønsted acidity of $0.2Sn_{SnCl_2}/Al_2O_3$–Cl is considerably greater than that of Al_2O_3–Cl (Table 3). On the other hand, the enhanced sum of the formation rates of ethylbenzene and styrene with the introduction of 0.2 wt% Sn from $SnCl_2$ (Table 4) might be consistent with protolytic cracking of *n*-PB. As already stated above, the Brønsted acidity also increases significantly with the introduction of 0.2 wt% Sn from $SnCl_2$ (Table 3). However, it must be emphasized that the sum of the formation rates of ethylbenzene and styrene is increased by only 50% with the introduction of Sn (Table 4), although the concentration of the strong Brønsted acid sites over $0.2Sn_{SnCl_2}/Al_2O_3$–Cl is about twice that over Al_2O_3–Cl (Table 2). Moreover, the protolytic cracking of *n*-PB must also favor the formation of benzene and toluene (Fig. 5), as the protonation of a C–H bond is supposed to occur preferentially on the most substituted carbon atom [32] or on a

carbon atom located in an α position with respect to a double bond [33], which is typically the case for the benzylic carbon atom of *n*-PB (Fig. 5a). However, in this study, we showed that toluene formation decreased (Table 4) when the Brønsted acidity of the Sn_{SnCl_2}/Al_2O_3–Cl catalyst increased (Table 3) compared with Al_2O_3–Cl. In addition to these arguments, it is important to emphasize that pure protolytic cracking is supposed to occur predominantly at conversion approaching zero [19,20,31,32], in the presence of low concentrations of olefins [34], because olefins are much better proton acceptors than alkanes [20,34,35], and at low partial pressure of hydrocarbons [19,32]. Let us recall that the present study was performed at conversions as high as 20%, in the presence of olefins [4] and with a rather high partial pressure of *n*-PB (0.8 bar).

4.2.3. Radical chemistry

As both carbenium ion and carbonium ion chemistries do not satisfactorily predict the formation of toluene and ethylbenzene or styrene from a mechanistic point of view, a radical-like cracking of *n*-PB was considered. Such radical pathways were suggested for the cracking of both alkyl aromatics and alkanes. As early as 40 years ago, Tung and McIninch [22] and Notari et al. [28] suggested radical mechanisms for the cracking of isopropylbenzene over high-purity alumina and that of toluene over alumina-modified catalysts, respectively. More recently, radical pathways have also been suggested to occur, to a significant extent, in the cracking of hexane isomers over H-mordenite [36], of *n*-butane over H-ZSM5 [30], and of *i*-butane over silica- and halided-alumina catalysts [29]. Although the last work was the subject of great controversy [37,38] by the defenders of the protolytic cracking mechanism [34,38]—most probably because the product distributions obtained by purely protolytic cracking and radical mechanisms are very similar [19]—recent reviews support the existence of radical mechanisms for the cracking of alkanes [19,33,39]. The initiation of the radical mechanism is assumed to occur over electron acceptor sites [19,36,37,39] such as Lewis acid sites [19,33,39].

Table 6 lists the sum of the formation rates of ethylbenzene and styrene and the formation rate of toluene together with the characterization of the Lewis acidity of the Sn/Al_2O_3–Cl catalysts. In this table, the sum of the amounts of medium and strong Lewis acid sites is also reported. It can be seen that the sum of the formation rates of ethylbenzene and styrene and the formation rate of toluene are fully correlated with the amounts of weak and medium–strong Lewis acid sites with the incorporation of Sn from $SnCl_2$ to a chlorided alumina (Table 6). Indeed, an increase in the sum of the formation rates of ethylbenzene and styrene and a decrease in the formation rate of toluene are linked to an increase in the amount of weak Lewis acid sites and a decrease in the medium–strong sites. These results thus suggest that these compounds are formed by a radical mechanism involving Lewis acid sites of different strengths. A very interesting theoretical work about the mechanism and the reactivity of alkane C–H bond dissociation on coordinatively unsaturated aluminum ions was recently published by Fărcaşiu and Lukinskas [40]. In this work, the authors showed that the reaction of propane over unsaturated aluminum ions, which typically correspond to Lewis acid sites, consisted of the insertion of an aluminum ion into the C–H bond, followed by hydrogen migration from Al to O to form the adsorbed intermediate. The elimination of hydrogen atoms from Cβ and oxygen then gives H_2 and propene. It is worth mentioning that such a detailed mechanism corroborates previous results suggesting that the presence of Lewis acid or electron acceptor sites of many acidic catalysts can enhance the dehydrogenation of paraffins [35,41–43]. Based on the work of Fărcaşiu and Lukinskas [40], the insertion of a C–H bond of *n*-PB located either on the benzylic carbon atom (Fig. 6a) or on the terminal carbon atom of the alkyl chain group (Fig. 7) is considered. In Figs. 6a and 7, for the sake of simplicity, the catalytic site is reduced to an Al–O pair with an unsaturated aluminum ion. Fig. 6a shows that the reactive adsorbate resulting from the adsorption of *n*-PB via the C–H bond of the benzylic carbon atom might be transformed via two different paths. Similar to Fărcaşiu and Lukinskas' proposal [40], the elimination of the hydrogen atom from Cβ leads to the formation of dehydrogenated compounds of *n*-PB and H_2 (catalytic cycle on the right side of Fig. 6a), whereas the radical C–Cβ scission leads to the formation of styrene and methane. The hydrogenation of styrene to ethylbenzene over Lewis acid sites (Fig. 6b), the reverse of the reaction proposed by Fărcaşiu and Lukinskas [40], requires the dissociation of H_2 over the catalytic site [44] and the reaction of these hydrogen atoms with a π-bonded molecule [40] of styrene. The hydrogenation of styrene can also be considered over the Brønsted acid sites with the protonation of styrene followed by a hydride transfer [18,19,24,34] from *n*-PB and the concurrent formation of a benzylic carbenium ion (Fig. 6c). The loss of a proton from this carbenium ion leads to the formation of the dehydrogenated products of *n*-PB and the restoration of the catalytic Brønsted acid site.

The existence of this hydrogenation path is supported by the work of Holm and Blue [45], who showed that ethylene

Table 6
Influence of the nature of the Sn precursor on the acidity of the catalysts and the sum of the formation rates of ethylbenzene and styrene, and the formation rate of toluene

	Catalysts		
	Al_2O_3–Cl	$0.2Sn_{SnCl_2}/Al_2O_3$–Cl	$0.2Sn_{SnBu_4}/Al_2O_3$–Cl
Formation rate (10^{-5} mol L^{-1} s^{-1})			
Ethylbenzene + styrene	2.3	3.6	3.2
Toluene	2.9	2.2	1.7
Lewis acidity (a.u.)			
Weak Lewis acid sites	1.98	2.22	1.43
Medium–strong Lewis acid sites	1.90	1.34	1.64

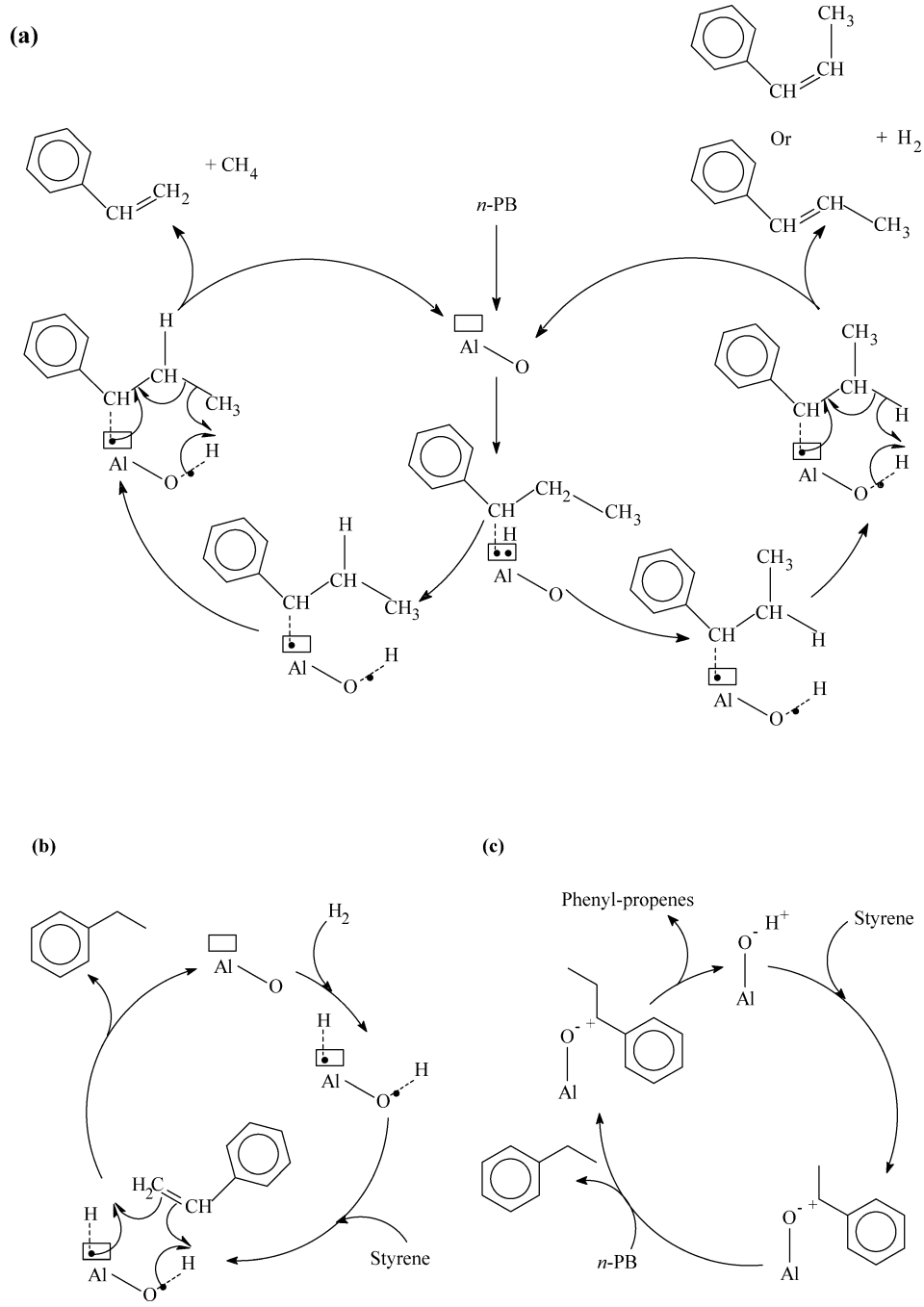

Fig. 6. (a) Proposed radical cracking and dehydrogenation of *n*-PB to styrene and E- and Z-phenyl-1-propene, respectively, over Lewis acid sites adapted from the work of Fărcaşiu and Lukinskas [40]; hydrogenation of styrene to ethylbenzene (b) over Lewis or (c) Brønsted acid sites.

could be almost fully hydrogenated to ethane over alumina at 500 °C. Comparable catalytic cycles such as those for the adsorption of *n*-PB via the benzylic carbon atom (Fig. 6a) are shown for the adsorption of *n*-PB by the terminal carbon atom of the alkyl chain (Fig. 7). In this case, the formation of phenyl-2-propene and H_2 (catalytic cycle on the right side of Fig. 7) and toluene and ethylene (catalytic cycle on the left side of Fig. 7) occurs.

Fărcaşiu and Lukinskas [40] also concluded that the insertion of the aluminum ion in the C–H bond was favored in the order prim C–H > *sec*-C–H > *tert*-C–H, which is in full agreement with the stability of the corresponding radical species. Considering this reactivity order of the C–H bonds, the lower formation of toluene compared with the sum of those of ethylbenzene and styrene (Table 6) might be surprising, as the formation of toluene involves the insertion of a prim C–H bond (Fig. 7), whereas that involved for the formation of ethylbenzene and styrene is a *sec*-C–H (Fig. 6a). However, in the case of *n*-PB, one must also consider the fact that the benzylic radical (Fig. 6a) is the most stable of the

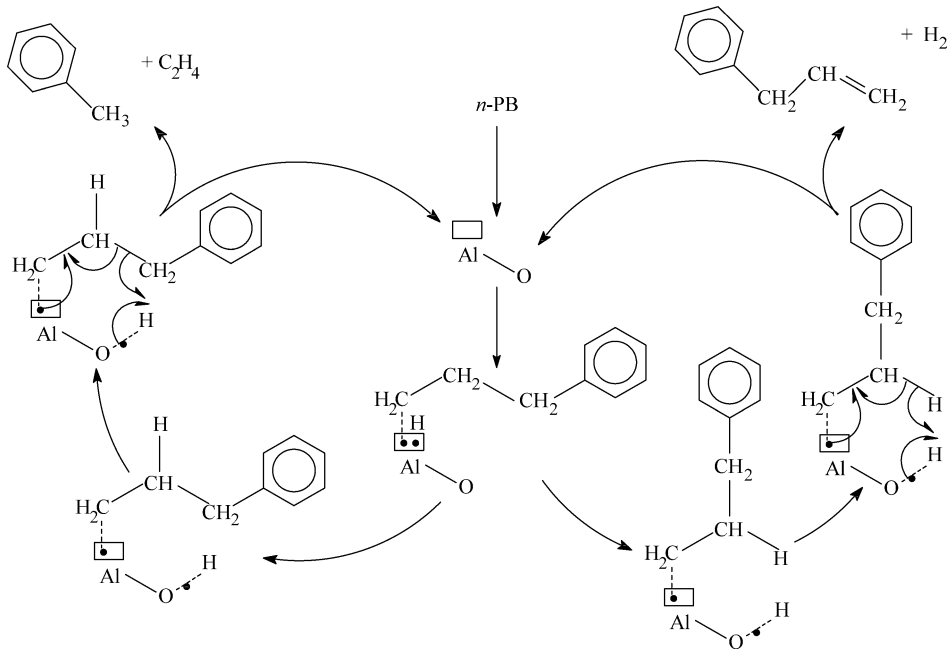

Fig. 7. Proposed radical cracking and dehydrogenation of *n*-PB to toluene and phenyl-2-propene, respectively, over Lewis acid sites adapted from the work of Fărcaşiu and Lukinskas [40].

above-mentioned radicals because it is resonantly stabilized by the aromatic ring [28]. This peculiarity therefore accounts for the higher formation of the sum of ethylbenzene and styrene than that of toluene for $0.2Sn_{SnCl_2}/Al_2O_3$–Cl compared with those found for Al_2O_3–Cl. It is also interesting to note that the stability of the speculated radicals is consistent with the strength of the Lewis acid sites assumed to be responsible for the formation of the two classes of product (Table 6). Indeed, the formation of the benzylic radical, involved in the formation of ethylbenzene or styrene (Fig. 6a), is more likely to occur on weaker Lewis acid sites than on those engaged in the formation of toluene, the radical intermediate of which (Fig. 7) is less stable than the benzylic radical intermediate. It must be added that the radical mechanisms suggested in the present study are nothing but radical C–C cleavages in the β position, as already proposed by Leveles et al. [46] for the oxidative conversion of propane.

Finally, Tung and McIninch [22] suggested an alternative path for the formation of toluene from isopropylbenzene with the intermediate isomerization of isopropylbenzene to *n*-PB, followed by decomposition of the 3-phenyl-propyl radical, which is identical to that proposed in the present work (catalytic cycle on the left side of Fig. 7).

The correlation with the Sn catalyst synthesized from $SnBu_4$ is less obvious than that with $0.2Sn_{SnCl_2}/Al_2O_3$–Cl (Table 6). However, the distribution of the acid strength of $0.2Sn_{SnBu_4}/Al_2O_3$–Cl is very close to that of Al_2O_3–Cl with a rather large proportion of medium Lewis acid sites (Table 3). In this case, the arbitrary desorption temperature range used for the assignment of the strength of the Lewis acid sites might not be adapted as done for that of $0.2Sn_{SnCl_2}/Al_2O_3$–Cl.

4.3. Influence of the content of Sn and the nature of the Sn precursor

Tables 4 and 5 clearly show that the content of Sn deposited on Al_2O_3–Cl and/or the nature of the Sn precursor do not evenly affect the production of the isomerized and cracked products and, thus, the acidity of the catalysts as shown in Table 3 for the $0.2Sn/Al_2O_3$–Cl materials.

For both series of supported Sn catalysts, the formation rates of the cracked compounds decrease with increasing Sn content (Tables 4 and 5). These results are consistent with a decrease in the acidity of the catalysts, as already reported in previous studies [7,8,12–14]. In contrast, the production of isopropylbenzene is almost constant for the Sn_{SnBu_4} series, whereas a maximum is obtained for the catalyst including 0.2 wt% Sn in the Sn_{SnCl_2} series. As suggested from the results of the present work, the production of isopropylbenzene and benzene occurs over the Brønsted acid sites via carbenium ion chemistry (Section 4.1). It is interesting to note that the ratio of the formation rate of isopropylbenzene to that of benzene increases with increasing Sn content for both series. A likely explanation for this trend is a decrease in the strength of the Brønsted acid sites with Sn addition. This explanation is consistent with previous studies that reported a decrease in the acidity of the support with the introduction of Sn, which resulted in higher selectivity for isomerization and lower selectivity for the cracking of C_6–C_8 alkanes over $PtSn/Al_2O_3$ catalysts [47–49]. The relative formation of toluene and ethylbenzene, attributed to Lewis acidity via radical chemistry, is also consistent with a decrease in the strength of the Lewis acid sites; the forma-

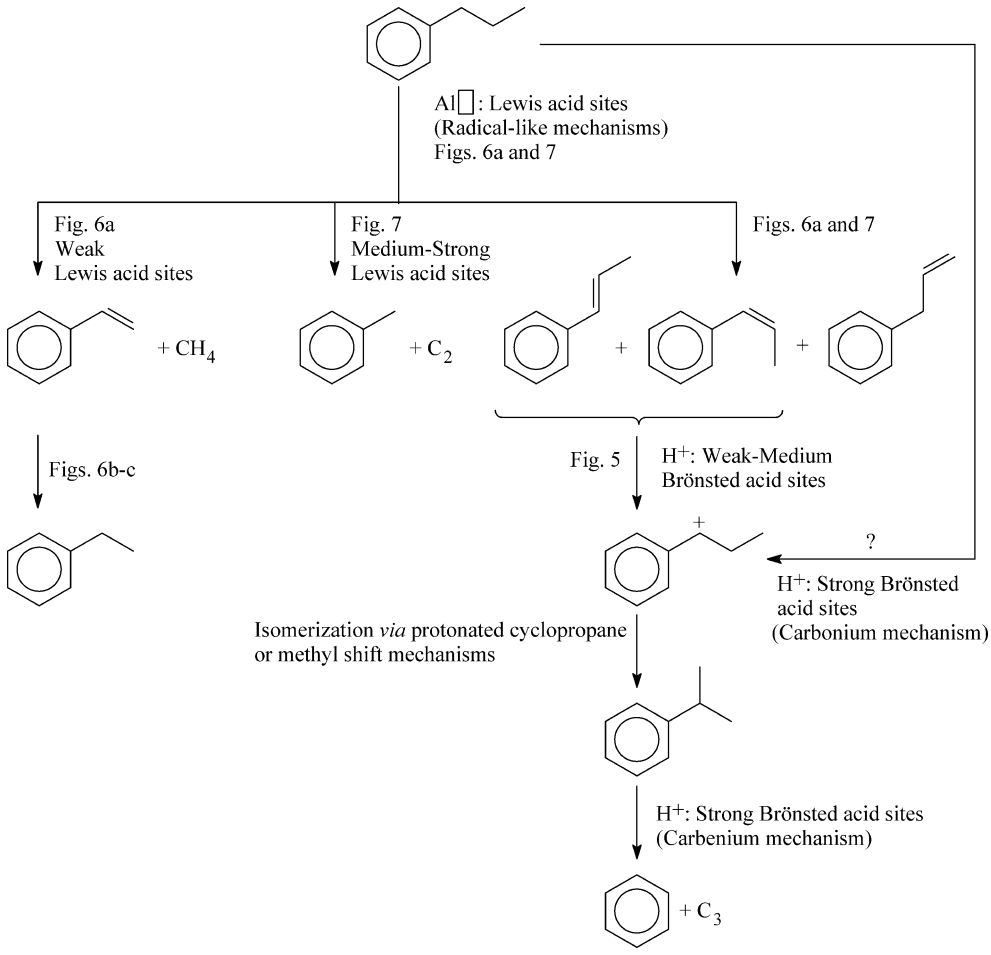

Fig. 8. Reaction network of the transformation of *n*-PB over chlorided alumina catalysts.

tion of toluene involves Lewis acid sites stronger than those needed for that of ethylbenzene (Section 4.2.3).

The comparison of the supported Sn catalysts with Al_2O_3–Cl is more complicated, and the main differences can be summarized as follows: (i) a drastic increase in the formation of isopropylbenzene over the Sn_{SnCl_2} series, whereas that of the Sn_{SnBu_4} series is not affected, and (ii) production of benzene promoted by the incorporation of Sn up to 0.2 wt% for the Sn_{SnCl_2} series, whereas benzene production is slightly inhibited for the Sn_{SnBu_4} series. This study therefore reveals that the incorporation of Sn via $SnCl_2$ strongly promotes Brønsted acidity for Sn contents of 0.2 wt% or less, whereas that via $SnBu_4$ does not significantly modify it. It must be emphasized that the promotional effect of Sn on the Brønsted acidity had not been stated up to now. The reasons for this are (i) most of the works investigated catalysts with Sn contents higher than 0.2 wt% [7,8,12,15,50]; (ii) for a Sn content of 0.11 wt%, the catalyst studied by Sheng et al. was chloride-free [13], whereas it is well known that the acidity of Al_2O_3 is promoted by the addition of Cl^- [51–53]; and (iii) the nature of the Sn precursor was rarely $SnCl_2$ [7]. It is thus clear that not only the content of Sn is important, but also the nature of the Sn precursor.

Finally, it is worth mentioning that benzene is always the major product of the cracked compounds for all of the catalysts investigated in the present work.

4.4. Reaction network of the transformation of n-PB over chlorided alumina acidic catalysts

The results discussed in the present study allowed us to propose the reaction network of the transformation of *n*-PB over chlorided alumina acidic catalysts shown in Fig. 8. This reaction network put a particular emphasis on the nature of the mechanisms involved in the formation of the different products and the nature and the strength of the required acid sites. It is quite interesting to note that ethylbenzene and toluene might be formed by radical monofunctional acidic pathways over the Lewis acid sites. The production of ethylbenzene involves Lewis acid sites weaker than those involved in the formation of toluene. In contrast, the formation of isopropylbenzene and benzene would be formed by bifunctional acidic mechanisms, as already suggested by Schuette and Schweizer [39]. Their production involves the intermediate formation of dehydrogenated products over the Lewis acid sites. These dehydrogenated compounds are then

catalytically converted to isopropylbenzene and benzene by the Brønsted acid sites. Following this reaction pathway, it is very likely that isopropylbenzene would require Brønsted acid sites weaker than those needed for the formation of benzene. This conclusion is in good agreement with basic cracking principles for which acid sites stronger than those needed for isomerization are required [18,49]. Although the existence of protolytic cracking of *n*-PB appears unlikely, its intervention as an initiation step to produce the benzylic carbenium ion shown in Fig. 8 cannot be ruled out.

5. Conclusion

Two series of chlorided alumina-supported Sn catalysts were synthesized with different precursors, $SnCl_2$ or $SnBu_4$, and with various Sn contents ranging from 0.1 to 0.5 wt%. The acidity of the catalysts including 0.2 wt% Sn was characterized by FTIR adsorption–desorption of 2,6-dimethylpyridine (Brønsted acidity) and pyridine (Lewis acidity) and compared with that of Al_2O_3–Cl. The catalytic activity of the synthesized materials was investigated for the transformation of *n*-propylbenzene under reforming conditions.

The results show that the incorporation of Sn into Al_2O_3–Cl is not harmless. Neither the nature of the Sn precursor nor the content of Sn evenly affects the acidity and the distribution of the isomerized and cracked products. Compared with Al_2O_3–Cl, the introduction of Sn from $SnBu_4$ slightly decreases the acidity of the materials and the production of benzene and toluene, whereas the production of isopropylbenzene remains constant and that of ethylbenzene increases slightly. In contrast, the incorporation of Sn from $SnCl_2$ drastically increases the Brønsted acidity; this effect is the most pronounced for Sn contents of 0.2 wt% or less. In addition, the incorporation of Sn from $SnCl_2$ decreases Lewis acidity very slightly.

The correlation between the product distribution obtained for the transformation of *n*-propylbenzene and the acidity of Al_2O_3–Cl and the $0.2Sn_{SnCl_2}/Al_2O_3$–Cl supports the formation of isopropylbenzene and benzene, catalyzed by Brønsted acid sites via carbenium ion chemistry. In contrast, the production of toluene and ethylbenzene cannot be attributed to carbenium ion or carbonium ion chemistries, but more likely to radical chemistry. The formation of these products is assumed to be catalyzed by Lewis acid sites with different strengths. The stability of the proposed radical intermediate species is consistent with the involvement of stronger Lewis acid sites for the production of toluene, compared with those involved for the production of ethylbenzene. The catalytic cycles responsible for the formation of toluene and ethylbenzene via radical pathways over an Al–O pair are reported. The correlation with the Sn catalyst synthesized from $SnBu_4$ is less obvious than the correlation with the Sn catalyst from $0.2Sn_{SnCl_2}/Al_2O_3$–Cl. However, the Lewis acid strength distribution of $0.2Sn_{SnBu_4}/Al_2O_3$–Cl is very close to that of Al_2O_3–Cl, with a rather large proportion of medium Lewis acid sites. In this case, the arbitrary desorption temperature range used for the assignment of the strength of the Lewis acid sites might not adapted as done for the sites of $0.2Sn_{SnCl_2}/Al_2O_3$–Cl.

Finally, it is worth noting that benzene is always the major product of the cracked compounds for all of the acidic catalysts investigated in the present work.

Acknowledgments

The Institut Français du Pétrole (IFP) provided financial support for this work; the ANRT organization supported the work of Ms. S. Toppi (CIFRE grant 128/99). We thank Dr. C. Marcilly (IFP) for fruitful discussions and for his interest in this work. Finally, we gratefully acknowledge P. Lavaud for technical support.

References

[1] B.H. Davis, Catal. Today 53 (1999) 443.
[2] J.H. Gary, G.E. Handwerk, in: L.F. Albright, R.N. Maddox, J.J. McKetta (Eds.), in: Petroleum Refining: Technology and Economics, vol. 5, Marcel Dekker, New York, 1975, p. 65.
[3] P.G. Menon, Z. Paál, Ind. Eng. Chem. Res. 36 (1997) 3282, and references therein.
[4] S. Toppi, C. Thomas, C. Sayag, D. Brodzki, F. Le Peltier, C. Travers, G. Djéga-Mariadassou, J. Catal. 210 (2002) 431.
[5] S. Toppi, C. Thomas, C. Sayag, D. Brodzki, F. Le Peltier, C. Travers, G. Djéga-Mariadassou, J. Catal. 218 (2003) 411.
[6] R. Burch, J. Catal. 71 (1984) 348.
[7] S.R. Bajaj, P. Pal, J.K. Gupta, L.D. Sharma, G. Murali Dhar, T.S.R. Prasada Rao, Stud. Surf. Sci. Catal. 113 (1998) 365.
[8] P. Kirszensztejn, B. Czajka, T.-C. Sheng, T.N. Bell, I.D. Gay, Catal. Lett. 32 (1995) 305.
[9] M. Moreno, A. Rosas, J. Alcaraz, M. Hernández, S. Toppi, P. Da Costa, Appl. Catal. A 251 (2003) 369.
[10] A. Corma, C. Rodellas, V. Fornes, J. Catal. 88 (1984) 374.
[11] A. Corma, V. Fornés, E. Ortega, J. Catal. 92 (1985) 284.
[12] P. Kirszensztejn, W. Przystajko, T.N. Bell, Catal. Lett. 18 (1993) 391.
[13] J. Shen, R.D. Cortright, Y. Chen, J.A. Dumesic, Catal. Lett. 26 (1994) 247.
[14] T.-C. Sheng, P. Kirszensztejn, T.N. Bell, I.D. Gay, Catal. Lett. 23 (1994) 119.
[15] D. Sprinceana, M. Caldararu, N.I. Ionescu, A. Auroux, J. Ther. Anal. Calor. 56 (1999) 109.
[16] L. Rodríguez, J. Alcaraz, M. Hernández, Y. Ben Taârit, M. Vrinat, Appl. Catal. A 189 (1999) 53.
[17] D. Best, B.W. Wojciechowski, J. Catal. 47 (1977) 11.
[18] Y.V. Kissin, Catal. Rev. 43 (2001) 85.
[19] A. Corma, A.V. Orchillés, Micropor. Mesopor. Mater. 35–36 (2000) 21.
[20] F.C. Jentoft, B.C. Gates, Topics Catal. 4 (1997) 1.
[21] C.D. Prater, R.M. Lago, Adv. Catal. 8 (1956) 295.
[22] S.E. Tung, E. McIninch, J. Catal. 4 (1965) 586.
[23] R. Covini, V. Fattore, N. Giordano, J. Catal. 7 (1967) 126.
[24] M. Guisnet, Stud. Surf. Sci. Catal. 20 (1985) 283.
[25] A. Corma, J.L.G. Fierro, R. Montana, F. Tomas, J. Mol. Catal. 30 (1985) 361.
[26] J. Weitkamp, Acta Phys. Chem. 31 (1985) 271.

[27] P.G. Smirniotis, E. Ruckenstein, Ind. Eng. Chem. Res. 34 (1995) 1517.
[28] B. Notari, P. Duranti, Valentini, M. Le Maldé, in: Proc. 3rd Congr. on Catalysis, Berlin, vol. 2, Verlag Chemie, Amsterdam, 1965, p. 1034.
[29] G.B. McVicker, G.M. Kramer, J.J. Ziemiak, J. Catal. 83 (1983) 286.
[30] Y.W. Bizreh, B.C. Gates, J. Catal. 88 (1984) 240.
[31] H. Krannila, W.O. Haag, B.C. Gates, J. Catal. 135 (1992) 115.
[32] W.O. Haag, R.M. Dessau, in: Proc. 8th Congr. on Catalysis, Berlin, vol. 2, Verlag Chemie, Weinheim, 1984, p. 305.
[33] A. Corma, Stud. Surf. Sci. Catal. 49 (1989) 49.
[34] S. Kotrel, H. Knözinger, B.C. Gates, Micropor. Mesopor. Mater. 35–36 (2000) 11.
[35] T.F. Narbeshuber, A. Brait, K. Seshan, J.A. Lercher, Appl. Catal. A 146 (1996) 119.
[36] D. Fărcaşiu, K.-H. Lee, J. Catal. 219 (2003) 186.
[37] G.M. Kramer, G.B. McVicker, J. Catal. 115 (1989) 608.
[38] W.K. Hall, E.A. Lombardo, J. Enghelardt, J. Catal. 115 (1989) 611.
[39] W.L. Schuette, A.E. Schweizer, Stud. Surf. Sci. Catal. 134 (2001) 263.
[40] D. Fărcaşiu, P. Lukinskas, J. Phys. Chem. A 106 (2002) 1619.
[41] S.E. Tung, E. McIninch, J. Catal. 10 (1968) 166.
[42] A. Brait, A. Koopmans, H. Weinstabl, A. Ecker, K. Seshan, J.A. Lercher, Ind. Eng. Chem. Res. 37 (1988) 873.
[43] T.F. Narbeshuber, A. Brait, K. Seshan, J.A. Lercher, J. Catal. 172 (1997) 127.
[44] D. Fărcaşiu, P. Lukinskas, J. Phys. Chem. A 103 (1999) 8483.
[45] V.C.F. Holm, R.W. Blue, Ind. Eng. Chem. 43 (1951) 501.
[46] L. Leveles, K. Seshan, J.A. Lercher, L. Lefferts, J. Catal. 218 (2003) 296.
[47] R. Burch, L.C. Garla, J. Catal. 71 (1981) 360.
[48] R. Bacaud, P. Bussière, F. Figueras, J. Catal. 69 (1981) 399.
[49] M.C. Rangel, L.S. Carvalho, P. Reyes, J.M. Parera, N.S. Figoli, Catal. Lett. 64 (2000) 171.
[50] R. Srinivasan, B.H. Davis, J. Mol. Catal. 88 (1994) 343.
[51] A. Ayame, G. Sawada, H. Sato, G. Zhang, T. Ohta, T. Izumizawa, Appl. Catal. 48 (1989) 25.
[52] T. Cai, S. Liu, J. Qü, S. Wong, Z. Song, M. He, Appl. Catal. A 97 (1993) 113.
[53] G. Clet, J.M. Goupil, G. Szabo, D. Cornet, J. Mol. Catal. 148 (1999) 253.